HHS Public Access

Author manuscript

J Phys Chem B. Author manuscript; available in PMC 2024 July 20.

Published in final edited form as:

J Phys Chem B. 2023 July 20; 127(28): 6241–6250. doi:10.1021/acs.jpcb.3c01426.

Amyloid Aggregation and Liquid-Liquid Phase Separation from the Perspective of Phase Transitions

Zhenzhen Zhang[1], **Gangtong Huang**[1], **Zhiyuan Song**[1], **Adam J. Gatch**[1,2], **Feng Ding**[1,*]

[1]Department of Physics and Astronomy, Clemson University, Clemson, SC 29634, United States

[2]Department of Genetics and Biochemistry, Clemson University, Clemson, SC 29634, United States

Abstract

Amyloid aggregation describes the aberrant self-assembly of peptides into ordered fibrils characterized by cross-β spine cores and is associated with many neurodegenerative diseases and type 2 diabetes. Oligomers, populated during the early stage of aggregation, are found to be more cytotoxic than mature fibrils. Recently, many amyloidogenic peptides have been reported to undergo liquid-liquid phase separation (LLPS) – a biological process important for the compartmentalization of biomolecules in living cells – prior to fibril formation. Understanding the relationship between LLPS and amyloid aggregation, especially the formation of oligomers, is essential for uncovering disease mechanisms and mitigating amyloid toxicity. In this perspective, available theories and models of amyloid aggregation and LLPS are first briefly reviewed. By drawing analogies to gas, liquid, and solid phases in thermodynamics, a phase diagram of protein monomer, droplet, and fibril states separated by coexistence lines can be inferred. Due to the high free energy barrier of fibrillization kinetically delaying the formation of fibril seeds out of the droplets, a “hidden” monomer-droplet coexistence line extends into the fibril phase. Amyloid aggregation can then be described as the equilibration process from the initial “out-of-equilibrium” state of a homogenous solution of monomers to the final equilibrium state of stable amyloid fibrils co-existing with monomers and/or droplets via the formation of metastable or stable droplets as the intermediates. The relationship between droplets and oligomers is also discussed. We suggest that the droplet formation of LLPS should be considered in future studies of amyloid aggregation, which may help to better understand the aggregation process and develop therapeutic strategies to mitigate amyloid toxicity.

Graphical Abstract

[*]Feng Ding, fding@clemson.edu.

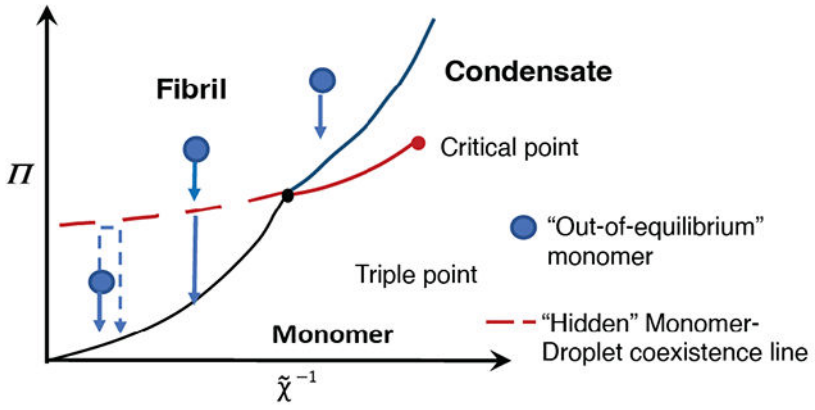

Keywords

liquid-liquid phase separation (LLPS); amyloid fibrillization; oligomer; droplet; phase diagram

Introduction

Amyloid fibrils are self-assembled protein aggregates that are characterized by their cross-β spine cores, which are comprised of tightly packed β-sheets with their β-strands aligned perpendicular to the fibril axis.[1–4] These protein aggregates are implicated in many diseases, including Alzheimer's disease, Parkinson's disease, and Type 2 diabetes, in which they accumulate and form extracellular plaques or intracellular inclusions.[5–7] Increasing evidence suggests that soluble aggregation intermediates play a greater role than mature fibrils in the pathology of amyloid diseases.[5,8] However, not all amyloid fibrils are associated with diseases. Functional amyloids have also been discovered in many organisms ranging from bacteria and fungi to mammals,[9] with biological roles including biofilm formation, adhesion, storage, and protection against stress.[9–13] Furthermore, the unique physicochemical properties of amyloid fibrils, including their high stability, unique mechanical properties, and biocompatibility, have led to their usage in an increasing range of nano-biomedical applications.[14–17]

Despite the diversity of amyloidogenic proteins, amyloid fibrils share common structural and kinetic properties. With recent advances such as cryo-electron microscopy (cryo-EM) and solid-state nuclear magnetic resonance (ssNMR) in structural biology, the fibrillar structures of many amyloid proteins have been solved.[18–21] The majority of these resolved fibrils are comprised of parallel in-register β-sheets, and fibrils formed by the same amyloid proteins may display distinct morphologies.[19,22–24] Amyloid proteins also share similar sigmoidal aggregation kinetics, characterized by rapid exponential-like growth following an initial lag phase, and then reaching a plateau due to saturation. A number of theories have been developed to describe the mechanisms of amyloid aggregation,[25] including the classical nucleation-dependent polymerization model, surface-catalyzed secondary nucleation and/or fragmentation, two-step nucleation, and the nucleated conformational conversion model.[26–30]

Recent studies have revealed that many amyloid proteins – e.g., α-synuclein,[31] tau,[32,33] islet amyloid polypeptide (IAPP),[34,35] amyloid-β (Aβ),[36] insulin A-chain fragment,[37] and TDP-43[38] – undergo liquid-liquid phase separation (LLPS) and form amyloid droplets prior to the formation of mature amyloid fibrils (e.g., Fig. 1). LLPS is a process by which a homogeneous solution can spontaneously separate into two phases, one rich in biomolecules and the other poor in biomolecules.[39,40] The resulting two phases have different physical properties, such as viscosity and diffusivity, and can be characterized as a dense phase and a dilute phase, respectively. LLPS plays a crucial role in the formation and maintenance of membraneless organelles, such as nucleoli[41] and stress granules.[42] A high concentration of amyloidogenic proteins in the droplets might promote the formation of toxic oligomers[43] and increase the nucleation rates for the formation of amyloid fibrils.[42,44] It has been postulated that LLPS could be a possible first step in the formation of amyloid fibrils.[35] However, since the conditions required for LLPS and amyloid fibril formation may differ, and the formation of droplets has not always been actively monitored in amyloid aggregation studies, and hence the relationship between LLPS and amyloid aggregation is still an active area of research.

In this perspective, we first briefly discuss available theories and models for amyloid aggregation and LLPS. We then draw analogies between LLPS and gas-liquid phase transition as well as between highly ordered amyloid fibrils and solid crystals. Analogous to the phase diagram of gas, liquid, and solid states, we infer a similar phase diagram for the amyloid protein monomer, droplet, and fibril states. Because of a high free energy barrier of fibrillization that kinetically delays the formation of fibrils, a dynamic "equilibrium" between monomers and droplets can be observed during fibrillization – i.e., the monomer-droplet coexistence line extends into the fibril phase. We propose that the formation of amyloid fibrils can then be described as the equilibration process from the initial "out-of-equilibrium" state of homogenous monomer solution to the final equilibrium state of stable amyloid fibrils co-existing with monomers and/or droplets via the formation of metastable or stable droplets as intermediates. Depending on the position of the initial "out-of-equilibrium" monomer state in the phase diagram, different aggregation pathways and kinetics are expected.

Amyloid aggregation

There are already many excellent reviews on amyloid aggregation theories and models in the literature.[25,45–47] Here, we only provide a brief overview of some of the major aggregation models.

The classical nucleation-dependent polymerization

In the classical nucleation-polymerization model, amyloid fibril growth is described by a single-step mechanism in which slow nucleation is followed by rapid growth. The protein concentration in the solution must reach a threshold known as the critical concentration in order for the fibril formation to occur.[48] Above the critical concentration, the soluble, monomeric proteins first undergo the nucleation process to form small aggregates, which then serve as a nucleus for further protein aggregation. After the critical nucleus size is

reached, the aggregation process becomes favorable, and the amyloid fibril begins to grow by further polymerization via monomer addition. The model explains the nucleation and subsequent polymerization, analogous to a homogeneous nucleation theory developed for vapor condensation.[49]

Fibril-dependent secondary nucleation and fragmentation

To capture the overall aggregation kinetics for a wide range of peptide concentrations, fibril-dependent secondary nucleation and fragmentation models have also been proposed. The secondary nucleation corresponds to the formation of an aggregation nucleus by monomers adsorbed on the lateral surface of newly formed fibrils, and the fragmentation of fibrils increases the number of active elongation sites for fibril growth. Fitting aggregation kinetics at different concentrations with closed-form analytical solutions under different nucleation scenarios has been successful for delineating the mechanisms of aggregation[26,27,50,51] and designing inhibitors.[46,52]

Supercritical concentration and the saturation of aggregation kinetics at high concentrations

The nucleated polymerization model predicts that the aggregation half-time decreases as protein concentration increases according to a strong power law dependence. However, such strong concentration dependence weakens and even disappears at high protein concentrations in experiments.[53] To account for the saturation of aggregation rates at high concentrations, Powers and Powers[54] pointed out the existence of a “supercritical concentration” above which the chemical potential of protein monomers in the solution is higher than that of these the critical nucleus. Hence, near and above this concentration, the fibril formation reaction behaves like an irreversible polymerization during the early stages, and the aggregation half-time becomes independent of the initial peptide concentration – i.e., the saturation of aggregation rates. In order to account for the accumulation of oligomers near and above the supercritical concentration of human islet amyloid polypeptide (hIAPP), Serrano et al. introduced to the kinetics model a free energy barrier between the oligomer and fibril states at a given nucleus size, corresponding to the refolding of oligomers into ordered fibrils.[29]

Two-step nucleation and nucleated conformational conversion

The two-step nucleation model describes the formation of amyloid fibrils in two distinct steps – first, amyloidogenic proteins self-assemble into prenucleation clusters, which then serve as seeds for the nucleation of amyloid fibrils.[28] Differing from the classical nucleation theory and its variants, where the proteins are basically treated as sticky objects without internal structures, the two-step model considers the nucleated conformational conversion of amyloid proteins that has been observed in experiments.[30,53] In the nucleated conformational conversion model, the fibrillization-competent protein structure is energetically unfavorable in the isolated monomeric state, but can be stabilized by extensive inter-peptide interactions in the fibrils. Using coarse-grained model that captured the nucleated conformational conversion, Saric et al.[28] showed that the critical nucleus size increases as both concentration and interpeptide interactions increase, in contrast to classical nucleation theory where the critical nucleus size is independent of peptide concentration.

Using either coarse-grained or atomistic simulations, several recent studies suggest that the self-assembly propensity of many intrinsically disordered amyloid proteins are encoded at the monomer level, where the fibrillization or LLPS-relevant conformations exist in the structural ensemble of monomers.[55–57]

Liquid-Liquid Phase Separation

In general, LLPS can be described by a mean-field Flory-Huggins theory for homopolymer solutions.[58,59] The LLPS of heteropolymers such as proteins can also be computationally modeled using coarse-grained simulations[60–62] or numerical modeling.[63,64]

Flory-Huggins Theory of Homopolymers

The Flory-Huggins theory considers the free energy change ΔF of mixing polymer and solvent, where both entropy and enthalpy are estimated according to mean-field approximations.[58,59] A dimensionless parameter, χ, is introduced to denote the net potential energy gain upon transferring a polymer composite unit from the solution into a pure polymer melt with respect to the thermal fluctuation energy k_BT, where k_B is the Boltzmann constant and T is the system temperature. Under certain conditions of the polymer-solvent interaction parameter χ, and the polymer concentration ϕ, the chemical potential of the polymer decreases with increasing polymer concentration (i.e., the second order derivative of free energy, $\partial^2 \Delta F / \partial \phi^2 \leq 0$), violating the second law of thermodynamics. Thus, the system spontaneously separates into two coexisting phases – a low-density phase where the polymers remain as non-interacting monomers, and a high-density phase where the loss of mixing entropy is compensated for by the potential energy gain due to interpolymer interactions (Fig. 2A). In the phase diagram of χ versus ϕ, the boundary with $\partial^2 \Delta F / \partial \phi^2 = 0$ forms the spinodal curve, and the concentrations of co-existing phases constitute the binodal curve. There exists a critical value of χ_c, which is approximately 1/2 for long polymers, below which polymers are effectively non-attractive and are completely miscible with the solvent at any concentration. It should be noted that $\chi_c \sim 1/2$ is a small value and the requirement for the transfer enthalpy gain (not free energy) out of the solvent greater than 0.5 k_BT can be easily satisfied,[65,66] making LLPS a ubiquitous self-assembly phenomenon in solution. For example, in crystallography proteins are known to form droplets first before crystallization occurs.[67]

Under a certain value of $\chi > \chi_c$, a horizontal line intersecting with the binodal and spinodal curves is called a tie line, which describes the phase behavior of the polymer-solvent system at a given temperature. At low polymer concentrations below the binodal point, the system is stable in a homogeneous low-density liquid phase. At higher concentrations between the binodal and spinodal points, an initially homogeneous system undergoes dynamic nucleation to form the polymer-rich high-density liquid phase. The classical nucleation-growth theory can be applied here to describe the phase separation process and the critical nucleus results from the competition between surface and bulk energies.[48] Above the spinodal point, the system will spontaneously undergo spinodal decomposition into two distinct phases, similar to the “supercritical concentration” phenomenon in the kinetics models proposed by Powers and Powers.[54] The local polymer concentration for each of the two phases is determined

only by the properties of both the polymer and solution, and changes to the total peptide concentration only result in changes of the partition of the two phases. Further increase of the polymer concentration to the second binodal and spinodal points results into the system entering the high-density phase as the dominant state and the low-density phase as the metastable state.

Modeling LLPS of Heteropolymeric Proteins

While the Flory-Huggins theory provides an excellent framework to describe the general properties of LLPS, it lacks the sequence dependence and residue-specific interactions of heteropolymeric proteins. It has been shown that the sequence properties are highly related to protein aggregation,[68] and the sequence information can be used to predict the formation of condensates in LLPS.[69] A *stickers-and-spacers* model, originally developed for associative polymers,[70] was proposed to divide protein sequences into interacting regions capable of multivalent linking (stickers) and the non- or weakly-interacting segments (spacers) separating the stickers.[71] Mutations in sticker, but not spacer regions, significantly altered the phase behavior of the UBQLN2 protein,[72] suggesting that the stickers are the main driving force for protein phase separation. Using an integrative approach combining biophysical experiments with multiscale simulations,[62] aromatic residues were found to function as stickers responsible for driving the LLPS of intrinsically disordered prion-like domains (PLDs) and a numerical stickers-and-spacers lattice model enabled accurate predictions of the corresponding binodal curve (Fig. 2B). In order to characterize the large molecular system of co-existing phases and the heterogeneity of protein sequences, coarse-grained (CG) off-lattice simulations have also been proven useful.[60–62,73] For example, in the *hydrophobicity scale model* (HPS), each residue is modeled as a CG bead and inter-residue interactions are assigned according to their relative hydrophobicity scales (Fig. 2C).[60] Combined with the slab simulation methodology,[74] the HPS model was able to generate the phase diagrams of large proteins, the dependence of LLPS on chain length and valence,[60] and describe mutation-induced changes of LLPS.[75] The hydrophobic scales of twenty amino acids was also optimized by the force-balance method on a library of proteins to reproduce their experimental radius of gyration, which resulted in a better prediction of LLPS under physiological conditions.[73] Recently, some higher-resolution models have also been developed to capture the thermodynamics of LLPS for intrinsically disordered proteins. Benayad et al. proposed an *adapted CG model* by rescaling inter-protein interactions in the MARTINI 2.2 force field to match the excess free energy of transferring proteins between dilute solution and condensate.[76] Paloni et al. adopted a “divide-and-conquer” strategy, based on atomistic molecular dynamics simulations of various protein fragments at high concentration, to probe the intermolecular interactions in conditions mimicking real condensates.[77]

LLPS and amyloid aggregation from the perspective of phase transitions

The phase diagram of amyloid protein monomer, droplet, and fibril states

LLPS is highly analogous to the gas-liquid phase transition. The phase diagram of chemical potential μ versus concentration ϕ for the mixed polymer solution in the Flory-Huggins theory (Fig. 2A) is also parallel to the pressure-volume (P-V) phase diagram of gas-liquid

phase transition for a simple Lenard-Jones system (Fig. 3A).[78] Under conditions where the increase of pressure results in volume increase, $\partial P/\partial V > 0$, violating the second law of Thermodynamics, the system spontaneously decomposes into two co-existing phases of gas and liquid. There is also a critical temperature, above which the gas and liquid phases become indistinguishable. For the supersaturated gas, liquid condensation also takes place via the formation of a critical nucleus.[79] With highly ordered and compact structures, amyloid fibrils can be regarded as the solid-like phase, although amyloid fibrils are structurally distinct from protein crystals[80] – e.g., amyloid fibrils are usually twisted along the fibril axis, and do not have the translational symmetry of crystals.

In LLPS, the entropy loss for the formation of amyloid protein droplets mainly results from the decrease in the number of translational degrees of freedom, and the conformational change is not considered in the Flory-Huggins theory. The height of the droplet nucleation barrier is, therefore, dependent on the monomer concentration. At sufficiently high monomer concentrations, the chemical potential of a peptide in the low-density phase can be higher than that in the critical droplet nucleus with the size of n_c^d.[54] In contrast, the nucleation of amyloid fibrils involves major conformational change from either intrinsically disordered or otherwise folded amyloid proteins to the fibrillar structure, leading to significant conformational entropy loss.[29] Especially for the nucleation of the critical fibril nucleus with the size of n_c^f, the cooperative “refolding” of multiple peptides into the fibril-like structure results into an exceedingly high free energy barrier, kinetically delaying the formation of fibril seeds out of the droplets. In general, the critical nucleus sizes for droplet formation n_c^d and fibrillization n_c^f are different. Since the peptide concentration of the droplets in equilibrium with monomers is constant according to the Flory-Huggins theory, the free energy barrier for the fibrillization nucleation is independent of the total peptide concentration. Once the fibril nuclei are formed, the conversion of monomers into the fibrillar state via elongation at fibril ends has a lower free energy barrier than fibril nucleation.

Similar to the pressure-temperature (P-T) phase diagram of gas, liquid and solid states, a phase diagram of amyloid protein monomer (Fig. 3B), droplet, and fibril states can then be inferred in terms of osmotic pressure Π and the effective Flory parameter $\tilde{\chi}$ (Fig. 3C). Here, osmotic pressure is analogous to pressure and the inverse of Flory parameter is proportional to temperature. For a dilute system like the low-density monomer phase, the osmotic pressure is proportional to the concentration. In the phase diagram, there is a triple point at which point the equilibrium coexistence lines of monomer-fibril, monomer-droplet, and droplet-fibril converge. However, due to the high fibril nucleation barrier, the monomer-liquid coexistence line can extend into the fibril phase temporarily (e.g., the red dash-line in Fig. 3C).

Fibrillization as the equilibration process from initial “out-of-equilibrium” monomer phase

Amyloid aggregation can then be regarded as the equilibration process from the initial “out-of-equilibrium” state of homogeneous monomers to stable states of amyloid fibrils co-existing with monomers and/or droplets via monomer-droplet, droplet-fibril, and monomer-fibril phase-transitions. In the phase diagram, this process corresponds to the relaxation

from a point in the fibril phase vertically back to the point intersecting with the fibril phase boundary, because $\tilde{\chi}$ is fixed for a polymer-solution at a given temperature. For most amyloidogenic proteins, the fibrils are highly stable under physiological conditions and there are few monomeric proteins remaining in the final solution, corresponding to the monomer-fibril equilibrium and suggesting a $\tilde{\chi}$ stronger than the triple point (e.g., cases 1 and 2 in Fig. 3C). Most amyloid fibrils only become unstable and disaggregate under high concentrations of denaturants,[81] representing reduced $\tilde{\chi}$ beyond the triple point or even the critical point (e.g., case 3 in Fig. 3C). Near the critical point of the monomer-droplet coexistence line, the critical opalescence due to long-range density fluctuations can be experimentally observed.[82]

When the initial monomer solution is below the hidden droplet-monomer coexistence line in the fibril phase (case 1 in Fig. 3C), the fibril seeds may still be nucleated out of the transiently formed droplets due to thermal fluctuations, and the fibrils grow mainly by monomer addition from the monomer phase. Equilibrium is reached when the chemical potential of the monomers is equal to that of the peptide composite of the fibrils. During the entire aggregation process, the droplet phase is metastable and only weakly populated (case 1 in Fig. 3D), and thus the classical nucleation theory may be a good approximation to describe the fibrillization kinetics. However, it should be noted that the probability of droplet formation and then fibril nucleation under this condition depends highly on the monomer concentration, and rapidly deceases with decreasing monomer concentration. When the initial monomer concentration is below a certain threshold, the spontaneous formation of fibrils may not occur and fibrillization can only take place with the addition of external fibril seeds.

If the “out-of-equilibrium” monomer is at higher concentrations above the hidden monomer-droplet coexistence line (e.g., case 2 in Fig. 3C), the high fibril nucleation barrier allows the system to quickly reach a “temporary” equilibrium of co-existing monomer and droplet phases (step I in Fig. 3D, case 2). Out of the droplets, fibril seeds are nucleated. Fibrils then grow by the addition of peptides from both monomer and droplet phases. As long as the droplets are not depleted, because of the relatively low free energy barrier of LLPS, the droplet-monomer equilibrium is expected to be maintained – i.e., the monomer concentration remains approximately the same and is *equal* to that of the binodal concentration (step II in Fig. 3D, case 2). Once the droplets are fully depleted, the fibrils grow by the addition of monomers and reach the monomer-fibril equilibrium (step III in Fig. 3D, case 2).

For a weakly sticky system with $\tilde{\chi}$ above the triple point, the initial monomer concentration should be high enough in order to be able form fibrils (e.g., case 3 in Fig. 3C). The system is expected to rapidly form a homogenous high-density protein solution phase, which further undergoes the droplet-fibril phase transition by nucleation and elongation. The final equilibrium has the fibrils co-exiting with the high-density, protein-rich solution state (Fig. 3D, case 3). Here, the high-density protein condensate is the dominant phase, and the term “droplet” might not be applicable to describe it.

CG simulations of fibrillization via LLPS

Using a coarse-grained peptide model that captured the nucleated conformational conversion and the capability of forming left-handed fibrils, we previously demonstrated that the amyloid aggregation below and above the spinodal concentration has the protein condensate as the metastable or stable intermediate state (Fig. 4A,B).[35] To distinguish the fibril nucleation from droplet nucleation, we computed the potential of mean force – i.e., the aggregation free energy landscape – as the function of both the aggregate size and the fraction of peptides forming fibrils (Fig. 4C). Indeed, the fibrillization process of the coarse-grained peptide undergoes LLPS as the initial step, followed by fibril nucleation inside the protein condensate, and then fibril growth by peptides from both the monomer and condensate phases (Fig. 4D), consistent with the equilibration process from the "out-of-equilibrium" state (Fig. 3).

In other CG simulations studying amyloid fibrillization,[28,83,84] the results can also be understood from the perspective of phase transitions. For instance, Barz and Urbanc[83] developed a simple tetrahedron model to study the self-assembly of ordered polymorphic fibril-like aggregates, in which the hydropathic ratio could be regarded as Flory-Huggins parameter χ and the initial formation of disordered, fluid-like small aggregates was reported. In the CG simulation by Saric et al.,[28] the observed two-step nucleation is consistent with the proposed amyloid fibrillization via LLPS as intermediate, where the "pre-fibrillar" oligomers can be regarded the droplet condensate. The observed increase of the critical nucleus size accompanying increases in both concentration and interpeptide interactions reflected the fact that an increase in either concentration (ϕ) or interpeptide interactions (χ) promoted LLPS and the fibril seeds were nucleated out of larger droplets. Adding another order parameter that distinguishes fibrils from the "pre-fibrillar" oligomers could separate the nucleation of droplets from the nucleation of amyloid fibrils.

Relationship between oligomers and droplets

The exact relationship or distinction between droplets and oligomers in amyloid aggregation remains elusive to date. The droplets of LLPS are usually stabilized by weak and non-specific interactions and the condensates are expected to be fluid-like and highly dynamic. Although the initially-formed protein droplets are nano-sized, they can grow into larger droplets (e.g., micronsized droplets in Fig. 1) via direct fusion or Ostwald Ripening[85] under favorable conditions when the initial monomer concentrations are above the spinodal point. In LLPS, the formation of droplets mainly reduces the translational entropy of the composite proteins without imposing major constraints on their internal conformational degrees of freedom. Hence, the weak interpeptide interactions probably have minimal impact on the secondary and tertiary structures of composite proteins, especially in the pristine droplets or within the liquid phase of droplets co-existing with the solid-like phase – i.e., fibrils or fibril seeds. In contrast, oligomers reported in the literature usually refer to those low-molecular-weight aggregates that are relatively long-lived, and stable enough to be separated/isolated with various experimental methods such as centrifuge and SDS-PAGE.[31] These oligomers are stabilized by extensive inter-peptide interactions, and have distinct structural features different from monomers.[86] Taken together, droplets and oligomers are expected to be different from each other in their sizes and composite protein structures

as well as the extent, strength and order of inter-protein interactions. We postulate that oligomers are not the nanodroplets formed in the process of LLPS; but likely correspond to the on- and off-pathway intermediates species formed during the nucleation of fibrils within the droplets. Protein droplets, on the other hand, provide a favorable environment for the formation of oligomers.

The formation of both droplets and oligomers during amyloid aggregation has be observed experimentally.[31] However, experimental characterizations of oligomers and droplets are usually done separately and under different conditions. To distinguish oligomers from droplets, it is important to measure them under the same condition and use experimental approaches with both high spatial and temporal resolutions – e.g., single-molecular fluorescence-based approaches that are able to differentiate the structure and dynamics of labeled peptides in liquid-like droplets versus more structurally ordered oligomers[31] or *in situ* liquid transmission electron microscopy.[87] Computationally, previous studies focused on fibrillization[28,35,83,84,88] and the distinction between droplets and oligomers remains to be explored *in silico*. The difference between oligomers and droplets in terms of the extent of inter-peptide interactions can be utilized to differentiate them. For example, different cutoffs in the number of inter-protein contacts and/or backbone hydrogen bonds can be used in the analysis of protein assemblies, and the corresponding cutoff values might be determined by probability distributions derived from simulations. Further computational and experimental studies are needed to uncover the exact relationship between oligomers and droplets, including these nanodroplets.[89]

Conclusion

The LLPS of proteins is analogous to the gas-liquid phase transition with monomers and droplet condensates corresponding to the gas and liquid phases, respectively. Despite the lack of translational symmetry, the ordered amyloid fibrils with cross-β spine cores can be regarded as the solid phase. Similar to the thermodynamics of gas, liquid, and solid, a phase diagram of amyloid protein monomer, condensate, and fibril states can be inferred. In addition to the critical point of LLPS, there is a triple point where the coexistence lines of monomer-droplet, monomer-fibril, and droplet-fibril converge. Due to a high free energy barrier of fibrillization kinetically delaying the nucleation of fibrils, the monomer-droplet coexistence line of LLPS extends into the fibril phase. Amyloid aggregation can then be described as the equilibration process from the initial “out-of-equilibrium” state of homogenous monomer solution to the final equilibrium state of stable amyloid fibrils co-existing with monomers and/or droplets via the formation of metastable or stable droplets as the intermediates. Depending on the position of the initial “out-of-equilibrium” monomer state in the phase diagram, different aggregation pathways and kinetics are expected. The sequence hydropathy heterogeneity might also drive the microphase separation inside the droplets, affecting the fibril nucleation and growth. The droplets are expected to be highly dynamic, undergo frequent exchanges with monomers in the solution, interact with each other and grow via direct fusion or Oswald Ripening.[85] These droplet intermediates, especially those that are nano-sized, can be experimentally challenging to characterize.[88] Future experimental and computational studies of amyloid aggregation should take droplet formation via LLPS into consideration to better understand the aggregation process, the

relationship between droplets and toxic oligomers, and to explore more efficient strategies to mitigate amyloid toxicity.

Acknowledgments

This work was supported in part by the NIH R35GM145409 and NIH P20GM121342. The content is solely the responsibility of the authors and does not necessarily represent the official views of the NIH.

Biographies

Zhenzhen Zhang is a Ph.D. candidate advised by Prof. Feng Ding in the Department of Physics and Astronomy at Clemson University, USA. She received her BSc degree from the Department of Physics at Nankai University in 2017. Her current research focuses on understanding early stage of amyloid aggregation, amyloid aggregation mitigation, RNA structure prediction, as well as RNA sequence design.

Gangtong Huang is a Ph.D. student at Clemson University. His research interests include using computational studies of amyloid disease etiology, functional amyloid aggregation, and protein/RNA design.

Zhiyuan Song is a Ph.D. candidate at Clemson University and a research assistant working under the supervision of Dr. Feng Ding. His research interests lie in elucidating the intricate interplay between protein structure, dynamics, and function, with a specific focus on studying the aggregation behavior of amyloid proteins and the cross-interactions that contribute to co-aggregation phenomena. His work aims to gain insights into the mechanisms underlying protein aggregation and its implications in various diseases.

Adam Gatch is an undergraduate student at Clemson University pursuing a B.S. in biochemistry. He is an undergraduate researcher in the department of Physics of Astronomy with interests in amyloid aggregation and protein-protein interactions in neurodegenerative diseases. Following graduation in 2025, he plans to pursue postgraduate education and continue to engage in biomedical research.

Feng Ding is a Professor of Physics at Clemson University, USA. He obtained his Ph.D. from Boston University (2004) and worked as a postdoctoral fellow (2004–2006), research associate (2006–2008), and Research Assistant Professor (2008–2012) at the University of North Carolina at Chapel Hill before being hired as an Assistant Professor at Clemson University (2012). His research focuses on understanding the structure, dynamics, and function interrelationship of biomolecules and molecular complexes. He was recipient of a Postdoctoral Award for Research Excellence (UNC, 2005), CAREER Award (US National Science Foundation, 2016), Outstanding Young Researcher (Clemson, 2017), Board of Trustee Award (Clemson, 2018), and Science Dean’s Distinguished Professorship (Clemson, 2021).

References

(1). Dobson CM; Dobson CM Protein Misfolding, Evolution and Disease. Trends Biochem. Sci 1999, 24 (9), 329–332. [PubMed: 10470028]

(2). Sunde M; Serpell LC; Bartlam M; Fraser PE; Pepys MB; Blake CCF Common Core Structure of Amyloid Fibrils by Synchrotron X-Ray Diffraction11Edited by F. E. Cohen. J. Mol. Biol 1997, 273 (3), 729–739. [PubMed: 9356260]

(3). Wiltzius JJW; Sievers SA; Sawaya MR; Cascio D; Popov D; Riekel C; Eisenberg D Atomic Structure of the Cross-β Spine of Islet Amyloid Polypeptide (Amylin). Protein Sci. 2008, 17 (9), 1467–1474. [PubMed: 18556473]

(4). Ke PC; Sani M-A; Ding F; Kakinen A; Javed I; Separovic F; Davis TP; Mezzenga R Implications of Peptide Assemblies in Amyloid Diseases. Chem. Soc. Rev 2017, 46 (21), 6492–6531. [PubMed: 28702523]

(5). Walsh DM; Selkoe DJ Aβ Oligomers – a Decade of Discovery. J. Neurochem 2007, 101 (5), 1172–1184. [PubMed: 17286590]

(6). Dauer W; Przedborski S Parkinson's Disease: Mechanisms and Models. Neuron 2003, 39 (6), 889–909. [PubMed: 12971891]

(7). DiFiglia M; Sapp E; Chase KO; Davies SW; Bates GP; Vonsattel JP; Aronin N Aggregation of Huntingtin in Neuronal Intranuclear Inclusions and Dystrophic Neurites in Brain. Science 1997, 277 (5334), 1990–1993. [PubMed: 9302293]

(8). Zraika S; Hull RL; Verchere CB; Clark A; Potter KJ; Fraser PE; Raleigh DP;Kahn SE Toxic Oligomers and Islet Beta Cell Death: Guilty by Association or Convicted by Circumstantial Evidence? Diabetologia 2010, 53 (6), 1046–1056. [PubMed: 20182863]

(9). Otzen D; Riek R Functional Amyloids. Cold Spring Harb. Perspect. Biol 2019, 11 (12), a033860. [PubMed: 31088827]

(10). Zeng G; Vad BS; Dueholm MS; Christiansen G; Nilsson M; Tolker-Nielsen T; Nielsen PH; Meyer RL; Otzen DE Functional Bacterial Amyloid Increases Pseudomonas Biofilm Hydrophobicity and Stiffness. Front. Microbiol 2015, 6, 1099. [PubMed: 26500638]

(11). Liu Y; Zhang Y; Sun Y; Ding F A Buried Glutamate in the Cross-β Core Renders β-Endorphin Fibrils Reversible. Nanoscale 2021, 13 (46), 19593–19603. [PubMed: 34812835]

(12). Guerette PA; Hoon S; Ding D; Amini S; Masic A; Ravi V; Venkatesh B; Weaver JC; Miserez A Nanoconfined β-Sheets Mechanically Reinforce the Supra-Biomolecular Network of Robust Squid Sucker Ring Teeth. ACS Nano 2014, 8 (7), 7170–7179. [PubMed: 24911543]

(13). Seuring C; Verasdonck J; Gath J; Ghosh D; Nespovitaya N; Wälti MA; Maji SK; Cadalbert R; Güntert P; Meier BH; et al. The Three-Dimensional Structure of Human β-Endorphin Amyloid Fibrils. Nat. Struct. Mol. Biol 2020, 27 (12), 1178–1184. [PubMed: 33046908]

(14). Cherny I; Gazit E Amyloids: Not Only Pathological Agents but Also Ordered Nanomaterials. Angew. Chem. Int. Ed Engl 2008, 47 (22), 4062–4069. [PubMed: 18412209]

(15). Ding D; Guerette PA; Hoon S; Kong KW; Cornvik T; Nilsson M; Kumar A; Lescar J; Miserez A Biomimetic Production of Silk-like Recombinant Squid Sucker Ring Teeth Proteins. Biomacromolecules 2014, 15 (9), 3278–3289. [PubMed: 25068184]

(16). Ding D; Pan J; Lim SH; Amini S; Kang L; Miserez A Squid Suckerin Microneedle Arrays for Tunable Drug Release. J. Mater. Chem. B 2017, 5 (43), 8467–8478. [PubMed: 32264514]

(17). Sun Y; Ding F Thermo- and PH-Responsive Fibrillization of Squid Suckerin A1H1 Peptide. Nanoscale 2020, 12 (11), 6307–6317. [PubMed: 32108838]

(18). Li Y; Zhao C; Luo F; Liu Z; Gui X; Luo Z; Zhang X; Li D; Liu C; Li X Amyloid Fibril Structure of α-Synuclein Determined by Cryo-Electron Microscopy. Cell Res. 2018, 28 (9), 897–903. [PubMed: 30065316]

(19). Cao Q; Boyer DR; Sawaya MR; Ge P; Eisenberg DS Cryo-EM Structure and Inhibitor Design of Human IAPP (Amylin) Fibrils. Nat. Struct. Mol. Biol 2020, 27 (7), 653–659. [PubMed: 32541896]

(20). Kollmer M; Close W; Funk L; Rasmussen J; Bsoul A; Schierhorn A; Schmidt M; Sigurdson CJ; Jucker M; Fändrich M Cryo-EM Structure and Polymorphism of Aβ Amyloid Fibrils Purified from Alzheimer's Brain Tissue. Nat. Commun 2019, 10 (1), 4760. [PubMed: 31664019]

(21). Wang L-Q; Zhao K; Yuan H-Y; Wang Q; Guan Z; Tao J; Li X-N; Sun Y; Yi C-W; Chen J; et al. Cryo-EM Structure of an Amyloid Fibril Formed by Full-Length Human Prion Protein. Nat. Struct. Mol. Biol 2020, 27 (6), 598–602. [PubMed: 32514176]

(22). Röder C; Kupreichyk T; Gremer L; Schäfer LU; Pothula KR; Ravelli RBG; Willbold D; Hoyer W; Schröder GF Cryo-EM Structure of Islet Amyloid Polypeptide Fibrils Reveals Similarities with Amyloid-β Fibrils. Nat. Struct. Mol. Biol 2020, 27 (7), 660–667. [PubMed: 32541895]

(23). Gallardo R; Iadanza MG; Xu Y; Heath GR; Foster R; Radford SE; Ranson NA Fibril Structures of Diabetes-Related Amylin Variants Reveal a Basis for Surface-Templated Assembly. Nat. Struct. Mol. Biol 2020, 27 (11), 1048–1056. [PubMed: 32929282]

(24). Kapurniotu A Enlightening Amyloid Fibrils Linked to Type 2 Diabetes and Cross-Interactions with Aβ. Nat. Struct. Mol. Biol 2020, 27 (11), 1006–1008. [PubMed: 33097922]

(25). Chatani E; Yamamoto N Recent Progress on Understanding the Mechanisms of Amyloid Nucleation. Biophys. Rev 2018, 10 (2), 527–534. [PubMed: 29214606]

(26). Knowles TPJ; Waudby CA; Devlin GL; Cohen SIA; Aguzzi A; Vendruscolo M; Terentjev EM; Welland ME; Dobson CM An Analytical Solution to the Kinetics of Breakable Filament Assembly. Science 2009, 326 (5959), 1533–1537. [PubMed: 20007899]

(27). šarić A; Michaels TCT; Zaccone A; Knowles TPJ; Frenkel D Kinetics of Spontaneous Filament Nucleation via Oligomers: Insights from Theory and Simulation. J. Chem. Phys 2016, 145 (21), 211926. [PubMed: 28799382]

(28). šarić A; Chebaro YC; Knowles TPJ; Frenkel D Crucial Role of Nonspecific Interactions in Amyloid Nucleation. Proc. Natl. Acad. Sci. U. S. A 2014, 111 (50), 17869–17874. [PubMed: 25453085]

(29). Serrano AL; Lomont JP; Tu L-H; Raleigh DP; Zanni MT A Free Energy Barrier Caused by the Refolding of an Oligomeric Intermediate Controls the Lag Time of Amyloid Formation by HIAPP. J. Am. Chem. Soc 2017, 139 (46), 16748–16758. [PubMed: 29072444]

(30). Lee J; Culyba EK; Powers ET; Kelly JW Amyloid-β Forms Fibrils by Nucleated Conformational Conversion of Oligomers. Nat. Chem. Biol 2011, 7 (9), 602–609. [PubMed: 21804535]

(31). Ray S; Singh N; Kumar R; Patel K; Pandey S; Datta D; Mahato J; Panigrahi R; Navalkar A; Mehra S; et al. α-Synuclein Aggregation Nucleates through Liquid-Liquid Phase Separation. Nat. Chem 2020, 12, 705–716. [PubMed: 32514159]

(32). Ambadipudi S; Biernat J; Riedel D; Mandelkow E; Zweckstetter M Liquid-Liquid Phase Separation of the Microtubule-Binding Repeats of the Alzheimer-Related Protein Tau. Nat. Commun 2017, 8 (1), 275. [PubMed: 28819146]

(33). Kanaan NM; Hamel C; Grabinski T; Combs B Liquid-Liquid Phase Separation Induces Pathogenic Tau Conformations in Vitro. Nat. Commun 2020, 11 (1), 2809. [PubMed: 32499559]

(34). Pytowski L; Lee CF; Foley AC; Vaux DJ; Jean L Liquid-Liquid Phase Separation of Type II Diabetes-Associated IAPP Initiates Hydrogelation and Aggregation. Proc. Natl. Acad. Sci. U. S. A 2020, 117 (22), 12050–12061. [PubMed: 32414928]

(35). Xing Y; Nandakumar A; Kakinen A; Sun Y; Davis TP; Ke PC; Ding F Amyloid Aggregation under the Lens of Liquid-Liquid Phase Separation. J. Phys. Chem. Lett 2021, 12 (1), 368–378. [PubMed: 33356290]

(36). Gui X; Feng S; Li Z; Li Y; Reif B; Shi B; Niu Z Liquid-Liquid Phase Separation of Amyloid-β Oligomers Modulates Amyloid Fibrils Formation. J. Biol. Chem 2023, 0 (0).

(37). Dec R; Jaworek MW; Dzwolak W; Winter R Liquid-Droplet-Mediated ATP-Triggered Amyloidogenic Pathway of Insulin-Derived Chimeric Peptides: Unraveling the Microscopic and Molecular Processes. J. Am. Chem. Soc 2023, 145 (7), 4177–4186.

(38). Babinchak WM; Haider R; Dumm BK; Sarkar P; Surewicz K; Choi J-K; Surewicz WK The Role of Liquid-Liquid Phase Separation in Aggregation of the TDP-43 Low-Complexity Domain. J. Biol. Chem 2019, 294 (16), 6306–6317. [PubMed: 30814253]

(39). Brangwynne CP; Eckmann CR; Courson DS; Rybarska A; Hoege C; Gharakhani J; Jülicher F; Hyman AA Germline P Granules Are Liquid Droplets That Localize by Controlled Dissolution/Condensation. Science 2009, 324 (5935), 1729–1732. [PubMed: 19460965]

(40). Shin Y; Brangwynne CP Liquid Phase Condensation in Cell Physiology and Disease. Science 2017, 357 (6357).

(41). Feric M; Vaidya N; Harmon TS; Mitrea DM; Zhu L; Richardson TM; Kriwacki RW; Pappu RV; Brangwynne CP Coexisting Liquid Phases Underlie Nucleolar Subcompartments. Cell 2016, 165 (7), 1686–1697. [PubMed: 27212236]

(42). Molliex A; Temirov J; Lee J; Coughlin M; Kanagaraj AP; Kim HJ; Mittag T; Taylor JP Phase Separation by Low Complexity Domains Promotes Stress Granule Assembly and Drives Pathological Fibrillization. Cell 2015, 163 (1), 123–133. [PubMed: 26406374]

(43). Elbaum-Garfinkle S Matter over Mind: Liquid Phase Separation and Neurodegeneration. J. Biol. Chem 2019, 294 (18), 7160–7168. [PubMed: 30914480]

(44). Lin Y; Protter DSW; Rosen MK; Parker R Formation and Maturation of Phase-Separated Liquid Droplets by RNA-Binding Proteins. Mol. Cell 2015, 60 (2), 208–219. [PubMed: 26412307]

(45). Ke PC; Zhou R; Serpell LC; Riek R; Knowles TPJ; Lashuel HA; Gazit E; Hamley IW; Davis TP; Fändrich M; et al. Half a Century of Amyloids: Past, Present and Future. Chem. Soc. Rev 2020, 49 (15), 5473–5509. [PubMed: 32632432]

(46). Arosio P; Vendruscolo M; Dobson CM; Knowles TPJ Chemical Kinetics for Drug Discovery to Combat Protein Aggregation Diseases. Trends Pharmacol. Sci 2014, 35 (3), 127–135. [PubMed: 24560688]

(47). Straub JE; Thirumalai D Toward a Molecular Theory of Early and Late Events in Monomer to Amyloid Fibril Formation. Annu. Rev. Phys. Chem 2011, 62, 437–463. [PubMed: 21219143]

(48). Oosawa F; 1922-; Asakura S; 1927-. Thermodynamics of the Polymerization of Protein; Academic Press, 1975.

(49). Ferrone F [17] Analysis of Protein Aggregation Kinetics. In Amyloid, Prions, and Other Protein Aggregates; Academic Press, 1999; Vol. Volume 309, pp 256–274.

(50). Michaels TCT; šarić A; Curk S; Bernfur K; Arosio P; Meisl G; Dear AJ; Cohen SIA; Dobson CM; Vendruscolo M; et al. Dynamics of Oligomer Populations Formed during the Aggregation of Alzheimer's Aβ42 Peptide. Nat. Chem 2020, 12 (5), 445–451. [PubMed: 32284577]

(51). Meisl G; Kirkegaard JB; Arosio P; Michaels TCT; Vendruscolo M; Dobson CM; Linse S; Knowles TPJ Molecular Mechanisms of Protein Aggregation from Global Fitting of Kinetic Models. Nat. Protoc 2016, 11 (2), 252–272. [PubMed: 26741409]

(52). Habchi J; Chia S; Limbocker R; Mannini B; Ahn M; Perni M; Hansson O; Arosio P; Kumita JR; Challa PK; et al. Systematic Development of Small Molecules to Inhibit Specific Microscopic Steps of Aβ42 Aggregation in Alzheimer's Disease. Proc. Natl. Acad. Sci. U. S. A 2017, 114 (2), E200–E208. [PubMed: 28011763]

(53). Serio TR; Cashikar AG; Kowal AS; Sawicki GJ; Moslehi JJ; Serpell L; Arnsdorf MF; Lindquist SL Nucleated Conformational Conversion and the Replication of Conformational Information by a Prion Determinant. Science 2000, 289 (5483), 1317–1321. [PubMed: 10958771]

(54). Powers ET; Powers DL The Kinetics of Nucleated Polymerizations at High Concentrations: Amyloid Fibril Formation Near and Above the "Supercritical Concentration." Biophys. J 2006, 91 (1), 122–132. [PubMed: 16603497]

(55). Dong X; Bera S; Qiao Q; Tang Y; Lao Z; Luo Y; Gazit E; Wei G Liquid-Liquid Phase Separation of Tau Protein Is Encoded at the Monomeric Level. J. Phys. Chem. Lett 2021, 12 (10), 2576–2586. [PubMed: 33686854]

(56). Chakraborty D; Straub JE; Thirumalai D Differences in the Free Energies between the Excited States of Aβ40 and Aβ42 Monomers Encode Their Aggregation Propensities. Proc. Natl. Acad. Sci. U. S. A 2020, 117 (33), 19926–19937. [PubMed: 32732434]

(57). Chakraborty D; Straub JE; Thirumalai D Energy Landscapes of Aβ Monomers Are Sculpted in Accordance with Ostwald's Rule of Stages. Sci. Adv 2023, 9 (12), eadd6921. [PubMed: 36947617]

(58). Flory PJ Thermodynamics of High Polymer Solutions. J. Chem. Phys 1942, 10 (1), 51–61.

(59). Huggins ML Solutions of Long Chain Compounds. J. Chem. Phys 1941, 9 (5), 440–440.

(60). Dignon GL; Zheng W; Kim YC; Best RB; Mittal J Sequence Determinants of Protein Phase Behavior from a Coarse-Grained Model. PLOS Comput. Biol 2018, 14 (1), e1005941. [PubMed: 29364893]

(61). Dignon GL; Zheng W; Best RB; Kim YC; Mittal J Relation between Single-Molecule Properties and Phase Behavior of Intrinsically Disordered Proteins. Proc. Natl. Acad. Sci 2018, 115 (40), 9929–9934. [PubMed: 30217894]

(62). Martin EW; Holehouse AS; Peran I; Farag M; Incicco JJ; Bremer A; Grace CR; Soranno A; Pappu RV; Mittag T Valence and Patterning of Aromatic Residues Determine the Phase Behavior of Prion-like Domains. Science 2020, 367 (6478), 694–699. [PubMed: 32029630]

(63). McCarty J; Delaney KT; Danielsen SPO; Fredrickson GH; Shea J-E Complete Phase Diagram for Liquid–Liquid Phase Separation of Intrinsically Disordered Proteins. J. Phys. Chem. Lett 2019, 10 (8), 1644–1652. [PubMed: 30873835]

(64). Borcherds W; Bremer A; Borgia MB; Mittag T How Do Intrinsically Disordered Protein Regions Encode a Driving Force for Liquid-Liquid Phase Separation? Curr. Opin. Struct. Biol 2021, 67, 41–50. [PubMed: 33069007]

(65). Wolfenden R; Andersson L; Cullis PM; Southgate CC Affinities of Amino Acid Side Chains for Solvent Water. Biochemistry 1981, 20 (4), 849–855. [PubMed: 7213619]

(66). Biswas KM; DeVido DR; Dorsey JG Evaluation of Methods for Measuring Amino Acid Hydrophobicities and Interactions. J. Chromatogr. A 2003, 1000 (1–2), 637–655. [PubMed: 12877193]

(67). Erdemir D; Lee AY; Myerson AS Nucleation of Crystals from Solution: Classical and Two-Step Models. Acc. Chem. Res 2009, 42 (5), 621–629. [PubMed: 19402623]

(68). Vendruscolo M; Fuxreiter M Sequence Determinants of the Aggregation of Proteins Within Condensates Generated by Liquid-Liquid Phase Separation. J. Mol. Biol 2022, 434 (1), 167201. [PubMed: 34391803]

(69). Horvath A; Vendruscolo M; Fuxreiter M Sequence-Based Prediction of the Cellular Toxicity Associated with Amyloid Aggregation within Protein Condensates. Biochemistry 2022, 61 (22), 2461–2469. [PubMed: 36341999]

(70). Semenov AN; Rubinstein M Thermoreversible Gelation in Solutions of Associative Polymers. 1. Statics. Macromolecules 1998, 31 (4), 1373–1385.

(71). Harmon TS; Holehouse AS; Rosen MK; Pappu RV Intrinsically Disordered Linkers Determine the Interplay between Phase Separation and Gelation in Multivalent Proteins. eLife 2017, 6, e30294. [PubMed: 29091028]

(72). Yang Y; Jones HB; Dao TP; Castañeda CA Single Amino Acid Substitutions in Stickers, but Not Spacers, Substantially Alter UBQLN2 Phase Transitions and Dense Phase Material Properties. J. Phys. Chem. B 2019, 123 (17), 3618–3629. [PubMed: 30925840]

(73). Dannenhoffer-Lafage T; Best RB A Data-Driven Hydrophobicity Scale for Predicting Liquid–Liquid Phase Separation of Proteins. J. Phys. Chem. B 2021, 125 (16), 4046–4056. [PubMed: 33876938]

(74). Blas FJ; MacDowell LG; de Miguel E; Jackson G Vapor-Liquid Interfacial Properties of Fully Flexible Lennard-Jones Chains. J. Chem. Phys 2008, 129 (14), 144703. [PubMed: 19045161]

(75). Monahan Z; Ryan VH; Janke AM; Burke KA; Rhoads SN; Zerze GH; O'Meally R; Dignon GL; Conicella AE; Zheng W; et al. Phosphorylation of the FUS Low-Complexity Domain Disrupts Phase Separation, Aggregation, and Toxicity. EMBO J. 2017, 36 (20), 2951–2967. [PubMed: 28790177]

(76). Benayad Z; von Bülow S; Stelzl LS; Hummer G Simulation of FUS Protein Condensates with an Adapted Coarse-Grained Model. J. Chem. Theory Comput 2021, 17 (1), 525–537. [PubMed: 33307683]

(77). Paloni M; Bailly R; Ciandrini L; Barducci A Unraveling Molecular Interactions in Liquid-Liquid Phase Separation of Disordered Proteins by Atomistic Simulations. J. Phys. Chem. B 2020, 124 (41), 9009–9016. [PubMed: 32936641]

(78). Reif F Fundamentals of Statistical and Thermal Physics, 56946th edition.; Waveland Pr Inc: Long Grove, Ill, 2008.

(79). Burton JJ Nucleation Theory. In Statistical Mechanics: Part A: Equilibrium Techniques; Berne BJ, Ed.; Modern Theoretical Chemistry; Springer US: Boston, MA, 1977; pp 195–234.

(80). Reynolds NP; Adamcik J; Berryman JT; Handschin S; Zanjani AAH; Li W; Liu K; Zhang A; Mezzenga R Competition between Crystal and Fibril Formation in Molecular Mutations of Amyloidogenic Peptides. Nat. Commun 2017, 8 (1), 1338. [PubMed: 29109399]

(81). Hirota-Nakaoka N; Hasegawa K; Naiki H; Goto Y Dissolution of Beta2-Microglobulin Amyloid Fibrils by Dimethylsulfoxide. J. Biochem. (Tokyo) 2003, 134 (1), 159–164. [PubMed: 12944383]

(82). Raut AS; Kalonia DS Pharmaceutical Perspective on Opalescence and Liquid-Liquid Phase Separation in Protein Solutions. Mol. Pharm 2016, 13 (5), 1431–1444. [PubMed: 27017836]

(83). Barz B; Urbanc B Minimal Model of Self-Assembly: Emergence of Diversity and Complexity. J. Phys. Chem. B 2014, 118 (14), 3761–3770. [PubMed: 24571643]

(84). Pellarin R; Caflisch A Interpreting the Aggregation Kinetics of Amyloid Peptides. J. Mol. Biol 2006, 360 (4), 882–892. [PubMed: 16797587]

(85). Yuan C; Yang M; Ren X; Zou Q; Yan X Porphyrin/Ionic-Liquid Co-Assembly Polymorphism Controlled by Liquid-Liquid Phase Separation. Angew. Chem. Int. Ed Engl 2020, 59 (40), 17456–17460. [PubMed: 32579296]

(86). Glabe CG Structural Classification of Toxic Amyloid Oligomers. J. Biol. Chem 2008, 283 (44), 29639–29643. [PubMed: 18723507]

(87). Le Ferrand H; Duchamp M; Gabryelczyk B; Cai H; Miserez A Time-Resolved Observations of Liquid-Liquid Phase Separation at the Nanoscale Using in Situ Liquid Transmission Electron Microscopy. J. Am. Chem. Soc 2019, 141 (17), 7202–7210. [PubMed: 30986043]

(88). Xing Y; Andrikopoulos N; Zhang Z; Sun Y; Ke PC; Ding F Modulating Nanodroplet Formation En Route to Fibrillization of Amyloid Peptides with Designed Flanking Sequences. Biomacromolecules 2022, 23 (10), 4179–4191. [PubMed: 36137260]

(89). Pittman JM; Srivastava AK; Boughter CT; Venkata BS; Zerweck J; Moore PC; Smok I; Tonelli M; Sachleben JR; Meredith SC Nanodroplet Oligomers (NanDOs) of Aβ40. Biochemistry 2021, 60 (36), 2691–2703. [PubMed: 34029056]

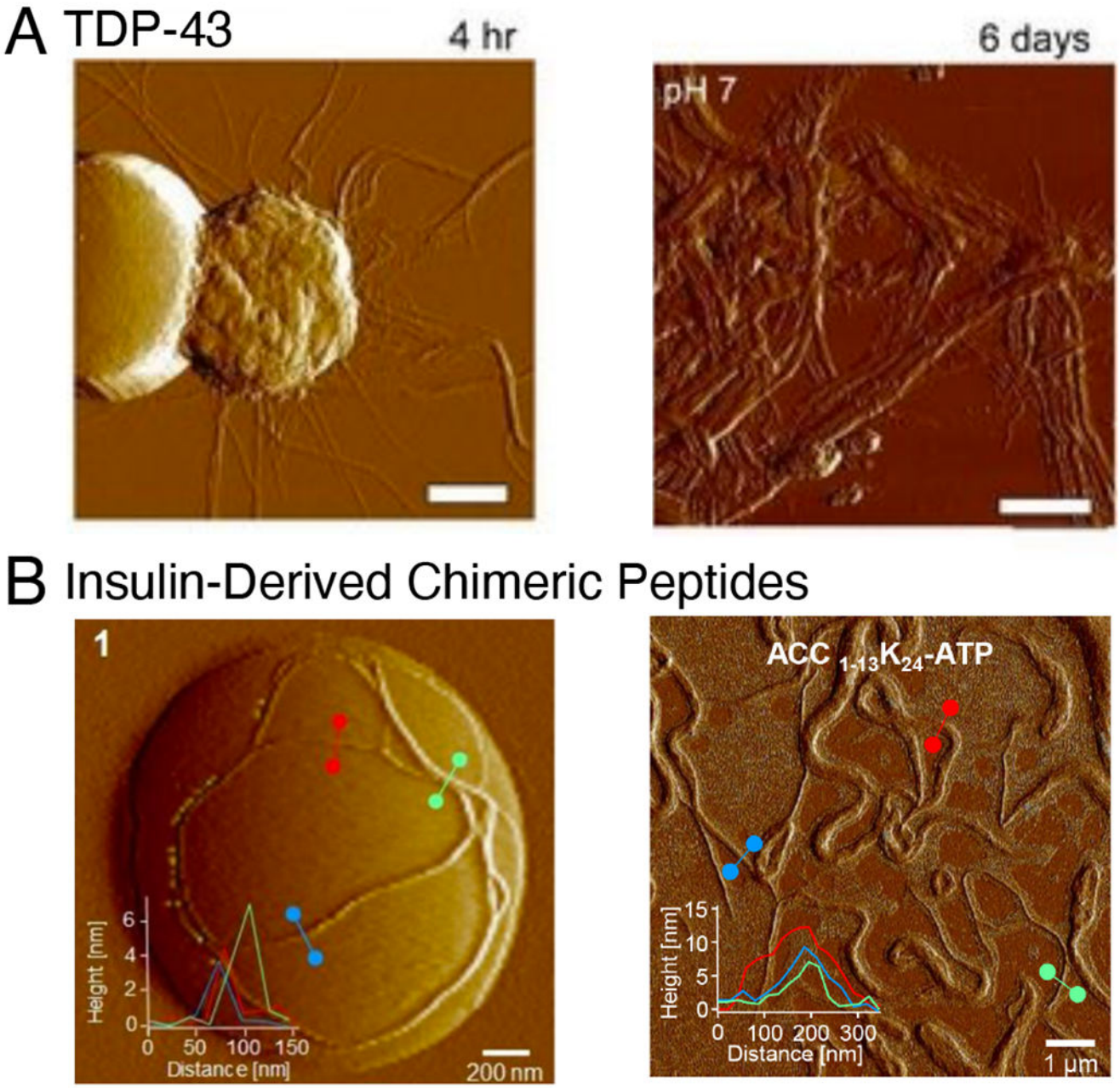

Figure 1.

Atomic force microscopy (AFM) imaging studies demonstrate the formation of amyloid fibrils out of the droplets for (A) TDP-43[38] and (B) insulin-derived chimeric peptide.[37] For both cases, the droplets were depleted and only fibrils were observed after long period of incubation. TDP-43 images are adapted with permission from Ref.[38]. Insulin-derived chimeric peptide images are adapted with permission from Ref.[37] Copyright 2023 American Chemical Society.

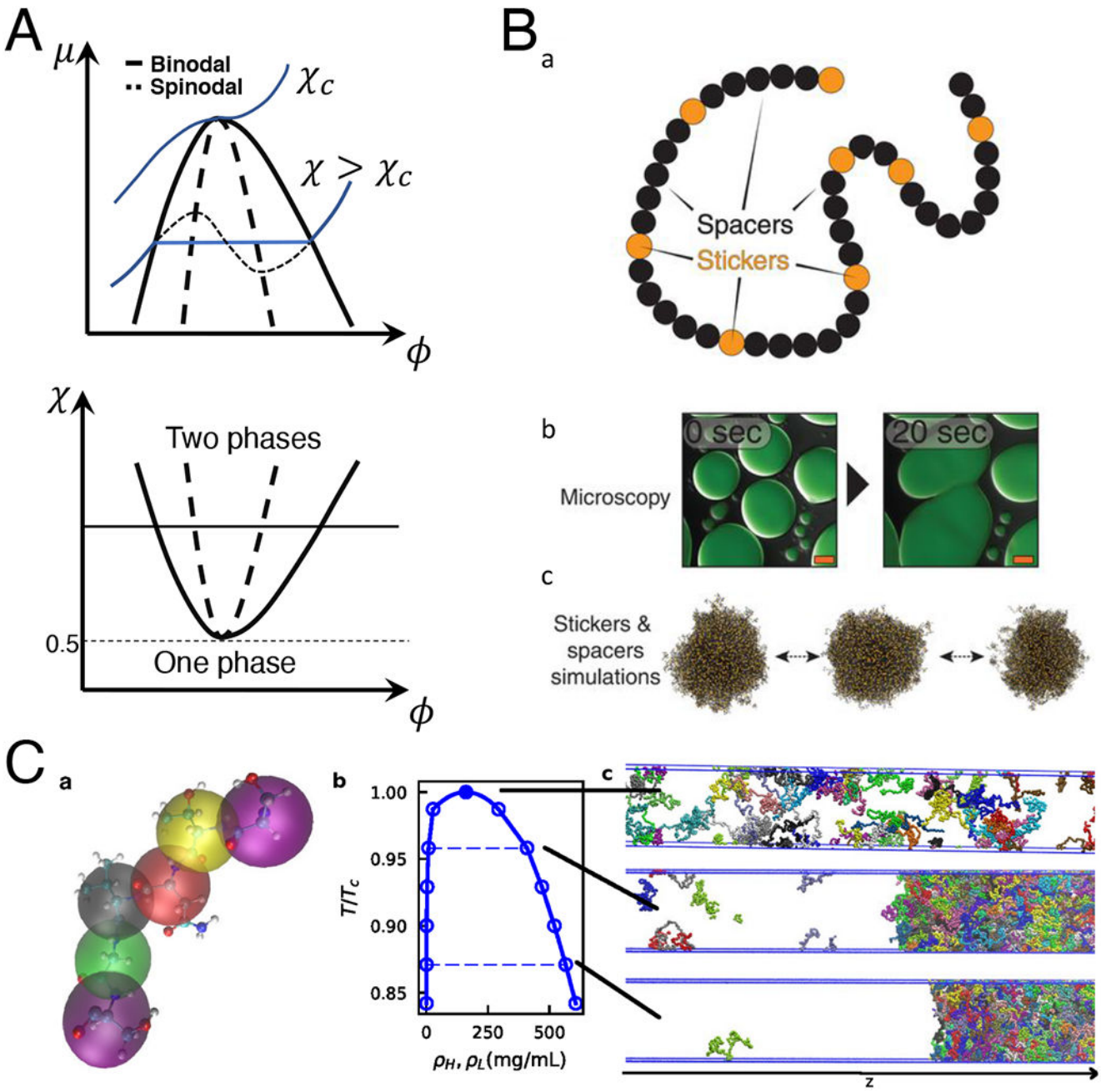

Figure 2.

Liquid-liquid phase separation modeling. (A) The chemical potential μ as the function of concentration ϕ for fully mixed polymer solution with different Flory parameter χ (blue lines, upper panel) according to the Flory-Huggins theory. The dash-line for $\chi > \chi_c$ denotes that the mixed system is either unstable (within the spinodal curve) or metastable (within the binodal curve). For a given polymer solution with a fixed χ, the equilibrium of the system with different total concentration can be described by the tie-line intersecting the binodal and spinodal curves (lower panel). (B) The stickers-and-spacers model used to describe the LLPS of prion-like domains (PLDs).[62] The sub-panel (a) denotes the schematic

representation of the model. The fluorescence images in sub-panel (b) demonstrates the fusion of droplets, which can be captured by lattice-based stickers-and-spacers simulations in subpanel (c). Adapted with permission from Ref.[62] Copyright 2020 The American Association for the Advancement of Science. (C) In the hydrophobicity scale (HPS) model, each amino acid is treated as a single particle (sub-panel a).[60] The binodal curve (sub-panel b) was obtained by slab simulations (sub-panel c). Adapted with permission from Ref.[60]

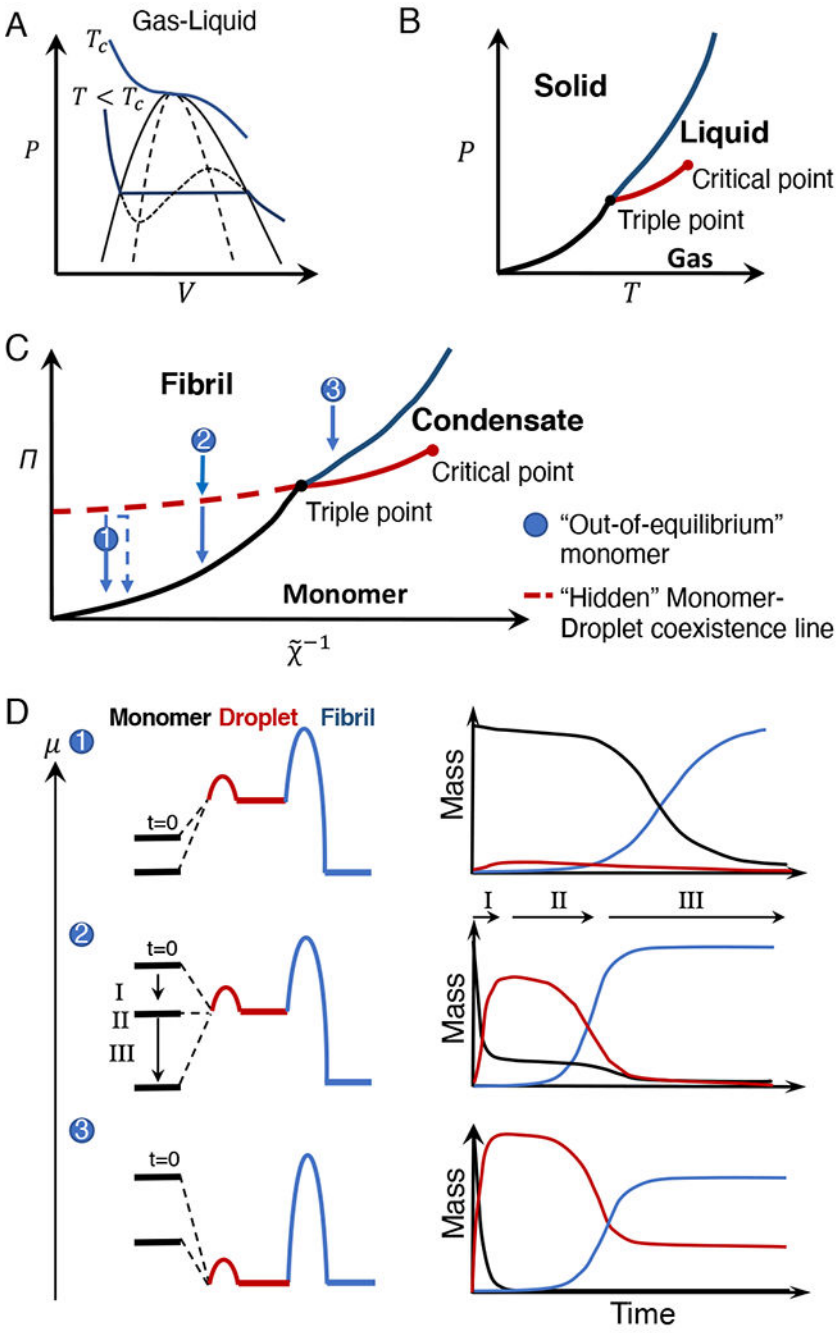

Figure 3.

Phase transitions and phase diagram. (A) The P-V phase diagram for the gas-liquid phase transition of a simple system interacting with Lenard-Jones potential.[78] (B) The P-T phase diagram of the gas, liquid, and solid. (C) The phase diagram of amyloid protein monomer, condensate, and fibril inferred in analogous to the phase diagram of gas, liquid, and solid. (D) For each of the three cases in panel C representing different positions of the "out-of-equilibrium" monomer state in the phase diagram, chemical potentials of a peptide in the monomer, droplet, and fibril phases are shown in the schematic diagram to the left for

different times during amyloid aggregation. The corresponding time-evolution of the mass concentration of three different phases is shown in the schematic diagram to the right.

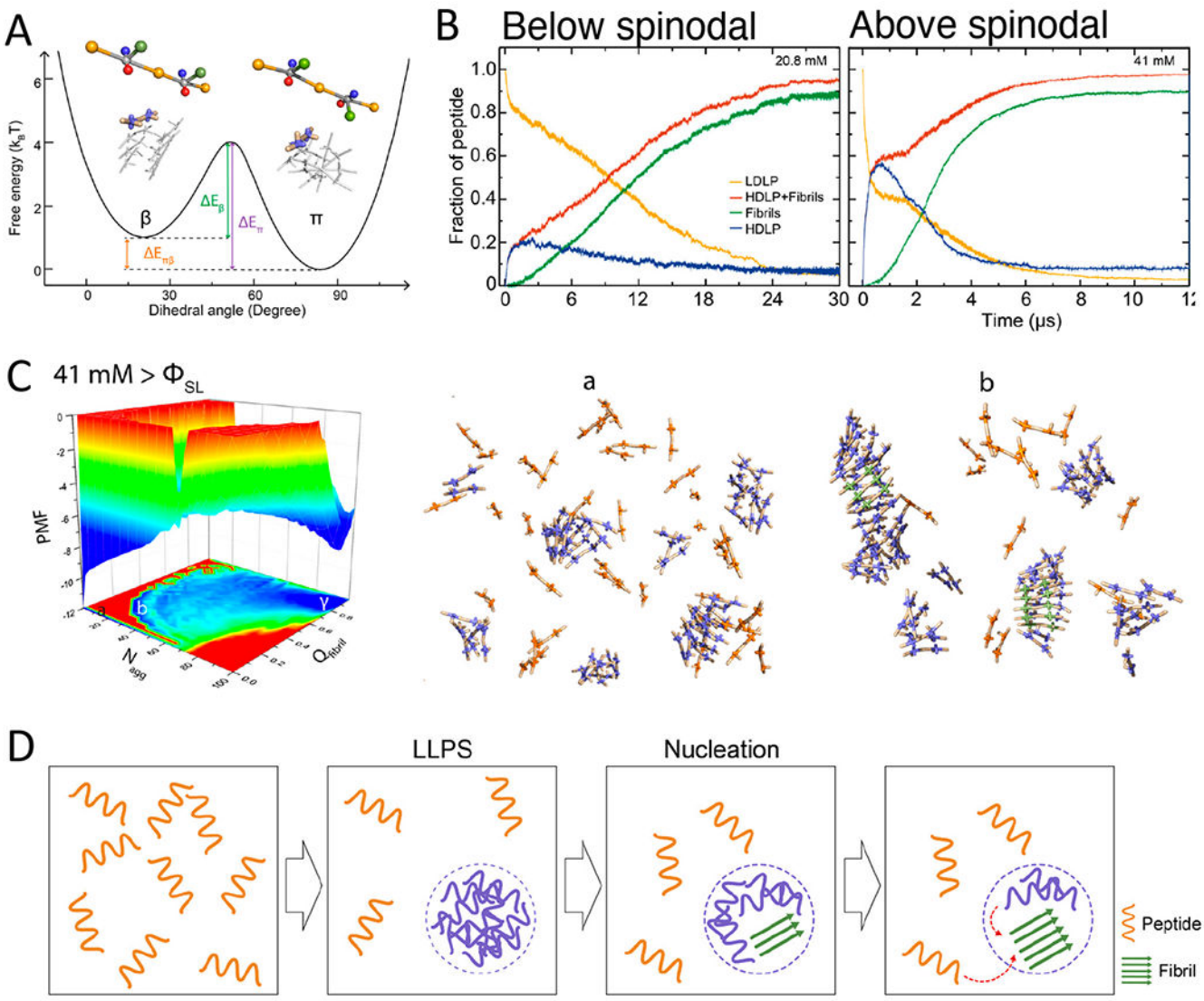

Figure 4.

Coarse-grained simulations of amyloid aggregation via LLPS as intermediates.[35] (A) The coarse-grained peptide model has two energy states, corresponding to the fibrillization-prone state β and fibrillization-incompetent state π shown in the inset. (B) The ensemble-averaged fraction of peptides in different components, including the monomers or low-density liquid phase (LDLP), the droplets or the high-density liquid phase (HDLP), and the fibrils and non-fibril aggregates in HDLP, as a function of time at concentrations blow (20.8 mM) and above (41 mM) of the spinodal point of ~25 mM. (C) The contour plo of the potential of mean force (PMF) is presented on the left as a function of the aggregate size (N_{agg}) and corresponding fraction of peptides forming fibrils (Q_{fibril}). Representative snapshots corresponding to the denoted basins in the 2D PMF are shown on the right, correspondingly. The peptides in monomers (orange), HDLP (purple), and fibrils (green) are shown in a stick representation. (D) Schematic diagram of the amyloid aggregation

mechanism through LLPS at high concentrations. Adapted with permission from Ref.[35] Copyright 2021 American Chemical Society.